Ratio Between Protection Coefficients and Oversized Coefficients for Pultruded Elements in Fire

Harkaitz García[1](✉), Aimar Insausti[1], Mikel Zubizarreta[2], and Iñaki Garmendia[1]

[1] Department of Mechanical Engineering, Faculty of Engineering Gipuzkoa, University of the Basque Country UPV/EHU, Plaza Europa (2018), Donostia-San Sebastián, Spain
arkaitz.garcia@ehu.eus

[2] Department of Business Organization, Faculty of Engineering Gipuzkoa, University of the Basque Country UPV/EHU, Plaza Europa (2018), Donostia-San Sebastián, Spain

Abstract. The main objective of the work presented is to provide a method to design the protection of pultruded elements in case of fire. The method is based on the development of tables similar to those already available for steel structures.

Using this table the designer will be able to calculate the protection to be given to each type of pultruded profile section based on its thickness and thermal conductivity. As a result it will be possible to obtain the specific over-dimensioning coefficient.

For the development of these tables, the maximum temperature restriction for class 4 sections has been applied, which is made in steel, but modified for pultruded sections based on the work carried out to date.

For this purpose, Eurocode 3 part 1–2 has been used to obtain the temperature in the section of each pultruded profile. Different properties of the pultruded material have been derived from experimental data carried out by other authors. Additionally, the mechanical properties and ultimate resistances of these profiles at different temperatures have also been obtained from previous literature.

Keywords: Pultruded elements · Fire protection · Dimensioning method · Class 4

1 Introduction

The main limitation of FRP profiles in building and bridge structures is their poor performance in cases of fire resistance needs as discussed by Wong et al. (2004), Bai and Keller (2009), Morgado et al. (2018a, b, c, d) and Rosa et al. (2018). But in spite of this, there must be some rules or standards for their design as there are with the rest of structural materials.

A. Ilki et al. (Eds.): CICE 2021, LNCE 198, pp. 753–762, 2022.
https://doi.org/10.1007/978-3-030-88166-5_65

One of the characteristics of pultruded FRP profiles is that most profiles could be classified within class 4, if the Eurocode 3 steel was followed (2005).

At room temperature, class 4 sections have different and more complex characteristics than the others (class 1, 2 and 3), due to the appearance of buckling within the section, which leads to specific rules in the design. These rules and their corresponding design methods are already established in the case of steel, Eurocode 3 (2005) and are being developed for pultruded elements, Ascione et al. (2016).

At higher temperatures (fire cases) the steel class 4 sections, in most buildings, can be said to be very over-dimensioned, Carlos et al. (2015, 2016), Martin et al. (2015) and Marcus et al. (2012), because they are limited to the critical temperature of 350 °C, when in reality it has been demonstrated that they could work at higher temperatures, Martin et al. (2016) and Jean et al. (2016).

To date, there are different countries with their own design guidelines for FRP structures, such as in the United States, A. C. M. Association et al. (2012), in Italy National Research Council (2007), in Germany BUEV-Guideline (2010) or in the Netherlands T. N. CUR Commission (2003), and none propose a specific procedure for the design at high temperatures. This does exist for the materials steel, Eurocode (1993), concrete, EHE-08 (2008) or wood, Eurocode (2004).

In the Eurocode for FRP being shaped, Ascione et al. (2016), to date, does not present specific design procedures in cases of fire requirements. This article proposes a design method for pultruded elements protected with RW, where tables are proposed to obtain the minimum insulation thickness necessary to achieve the required mechanical properties of the section.

Fire resistance times down to 60 min have been recorded in these tables, as it has been concluded during the development of the tables that longer exposure times are not feasible, for reasonable coating thicknesses.

Furthermore, these tables have not been limited to the standard 30, 60, 90 min times, but have been discrete in shorter times. From 5 min to 60 min in 5-min increments.

It is considered that this discretization of times can be useful to optimize the structures in case of fire, as long as the adjustment of the standard times of requirement is made by means of its specific calculation. For example, using the standard formula of the equivalent time, Eurocode (2002).

2 Methodology

The steps taken to achieve the tables proposed in the design method outlined in this article will be explained below (Fig. 1):

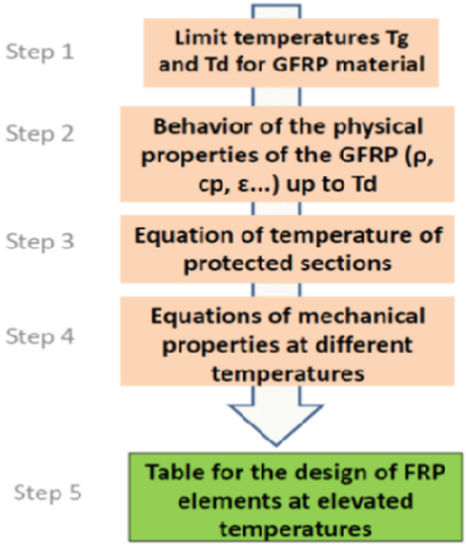

Fig. 1. Methodology for the development of the tables.

In step 1, you have searched for items where you specify the limit temperature up to which it is possible to use the FRP material for structures.

As commented by Bai and Keller (2007), the modulus of elasticity suffers a considerable decrease (although recoverable) during its glass transition Tg, but in addition, although the longitudinal and transversal modulus of elasticity are different in this material, the decrease they suffer is similar in the stretch between Tg and Td, Bai et al. (2008a, b).

That is why the existing guidelines limit the use of FRPs to temperatures close to Tg. Taking as a reference the data of the common FRP used in Morgado et al.'s work (2018a, b, c, d) (Tg = 141 °C, Td = 370 °C) the temperature limits of these guides would be as follows:

– ASCE: Tg-22 = 141 – 20 = 119 ºC
– German guideline: Tg-15 = 141 – 20 = 126 °C
– Dutch: Tg-20 = 141 – 20 = 121 °C

Tg, media aprox = 120 °C.

In the specific design procedure for FRP structures proposed in this article, three design ranges have been considered depending on the temperature achieved by the profile:

– Zone 1 (green): Ts (section temperature) < 120 °C
– Zone 2 (yellow): 120 °C < Ts (section temperature) < 370 °C
– Zone 3 (red): Ts (section temperature) > 370 °C

In zone 1 it is possible to calculate the structures without modifying their elastic modulus. In zone 2 the elastic modulus should be corrected using the one corresponding to the actual temperature of the section. To obtain the modulus of elasticity, the equation proposed by Bai et al. (2008a, b) is proposed (Eq. 1). Finally, it is not advisable to design FRP structures within the range corresponding to zone 3.

$$\mathrm{Em} = \mathrm{Eg} \cdot (1 - \alpha\mathrm{g}) + \mathrm{Er} \cdot \alpha\mathrm{g} \cdot (1 - \alpha\mathrm{g}) \tag{1}$$

where Em is the modulus of elasticity, Eg and Er are the glassy and rubbery modulus, respectively, and αg is the conversion degree of the glass transition (Fig. 2).

30 m⁻¹		time (min)											
δ/λx	d	6	10	16	20	26	30	36	40	46	60	66	80
0.06	0.002	73.84	145.08	217.05	286.26	351.45	412.16	468.32	520.06	567.60	611.20	651.16	687.77
0.1	0.004	47.32	85.71	126.66	168.25	209.57	250.16	289.73	328.11	365.20	400.94	435.33	468.35
0.16	0.006	38.04	64.22	92.70	122.16	152.00	181.85	211.49	240.76	269.58	297.86	325.55	352.62
0.2	0.008	33.27	53.09	74.87	97.63	120.91	144.41	167.97	191.46	214.80	237.91	260.76	283.30
0.26	0.01	30.35	46.24	63.85	82.37	101.42	120.77	140.27	159.83	179.38	198.85	218.20	237.40
0.3	0.012	28.36	41.59	56.35	71.94	88.04	104.46	121.09	137.82	154.61	171.40	188.14	204.83
0.36	0.014	26.91	38.22	50.90	64.34	78.27	92.53	107.00	121.61	136.30	151.04	165.78	180.51
0.4	0.016	25.81	35.65	46.75	58.55	70.82	83.40	96.20	109.16	122.21	135.34	148.50	161.66
0.46	0.018	24.93	33.62	43.47	53.99	64.94	76.19	87.66	99.29	111.03	122.85	134.72	146.62
0.6	0.02	24.23	31.98	40.82	50.29	60.17	70.34	80.72	91.26	101.92	112.67	123.48	134.33
0.66	0.022	23.64	30.62	38.63	47.23	56.22	65.49	74.97	84.61	94.36	104.21	114.13	124.10
0.8	0.024	23.15	29.48	36.79	44.65	52.90	61.41	70.12	78.99	87.98	97.07	106.22	115.44

60 m⁻¹		time (min)											
δ&x	d	6	10	16	20	26	30	36	40	46	60	66	80
0.06	0.002	106.39	213.89	314.97	405.71	485.63	555.39	616.04	668.71	714.48	754.32	789.10	819.58
0.1	0.004	64.69	125.44	187.97	249.22	307.94	363.60	415.97	465.04	510.86	553.56	593.30	630.25
0.16	0.006	49.66	91.79	136.52	181.70	226.34	269.93	312.17	352.92	392.07	429.59	465.48	499.76
0.2	0.008	41.89	74.02	108.73	144.33	180.07	215.51	250.38	284.53	317.83	350.23	381.68	412.15
0.26	0.01	37.08	62.99	91.28	120.59	150.30	180.04	209.58	238.77	267.51	295.73	323.36	350.39
0.3	0.012	33.81	55.44	79.27	104.14	129.52	155.09	180.65	206.07	231.25	256.13	280.64	304.76
0.36	0.014	31.42	49.93	70.49	92.06	114.17	136.57	159.06	181.53	203.89	226.08	248.05	269.76
0.4	0.016	29.59	45.73	63.77	82.79	102.36	122.26	142.32	162.43	182.51	202.51	222.37	242.07
0.46	0.018	28.15	42.41	58.45	75.44	92.98	110.87	128.95	147.13	165.34	183.52	201.63	219.63
0.6	0.02	26.98	39.71	54.13	69.46	85.34	101.57	118.02	134.59	151.23	167.88	184.50	201.07
0.66	0.022	26.00	37.47	50.55	64.50	78.99	93.83	108.90	124.13	139.43	154.78	170.13	185.46
0.8	0.024	25.19	35.59	47.53	60.31	73.62	87.28	101.18	115.25	129.41	143.64	157.89	172.14

100 m⁻¹		time (min)											
δ/λx	d	6	10	16	20	26	30	36	40	46	60	66	80
0.06	0.002	178.75	346.46	480.56	583.81	662.90	723.94	771.72	809.80	840.76	866.45	888.19	906.94
0.1	0.004	105.36	212.33	313.24	403.91	483.84	553.65	614.39	667.16	713.04	752.99	787.89	818.48
0.16	0.006	77.41	154.66	231.99	305.62	374.24	437.50	495.43	548.28	596.37	640.09	679.81	715.89
0.2	0.008	62.61	122.73	184.83	245.77	304.28	359.78	412.06	461.08	506.90	549.63	589.42	626.43
0.26	0.01	53.36	102.38	154.05	205.72	256.23	305.03	351.81	396.44	438.87	479.10	517.18	553.17
0.3	0.012	46.99	88.24	132.35	177.05	221.30	264.57	306.57	347.11	386.11	423.52	459.33	493.56
0.36	0.014	42.33	77.81	116.21	155.49	194.76	233.50	271.44	308.38	344.23	378.90	412.38	444.65
0.4	0.016	38.75	69.78	103.70	138.68	173.90	208.90	243.40	277.22	310.25	342.42	373.67	403.99
0.46	0.018	35.91	63.39	93.71	125.19	157.07	188.92	220.50	251.62	282.17	312.07	341.28	369.75
0.6	0.02	33.61	58.18	85.54	114.10	143.18	172.37	201.44	230.21	258.57	286.46	313.80	340.57
0.66	0.022	31.69	53.84	78.71	104.83	131.52	158.43	185.32	212.03	238.47	264.55	290.21	315.42
0.8	0.024	30.09	50.17	72.93	96.94	121.59	146.51	171.51	196.41	221.14	245.60	269.74	293.52

160 m⁻¹		time (min)											
δ&x	d	6	10	16	20	26	30	36	40	46	60	66	80
0.06	0.002	238.89	437.52	574.78	668.46	734.02	781.76	818.08	846.90	870.64	890.79	908.33	923.89
0.1	0.004	142.39	284.04	407.00	509.03	592.48	660.54	716.18	761.96	799.95	831.78	858.76	881.88
0.16	0.006	103.38	209.78	310.40	400.96	480.88	550.78	611.65	664.59	710.64	750.79	785.87	816.63
0.2	0.008	82.24	166.69	250.25	328.79	401.07	466.86	526.38	580.04	628.32	671.73	710.76	745.88
0.26	0.01	68.87	138.52	209.45	277.96	342.69	403.12	459.17	510.92	558.56	602.34	642.54	679.44
0.3	0.012	59.60	118.63	179.98	240.38	298.48	353.70	405.80	454.71	500.49	543.24	583.09	620.21
0.36	0.014	52.77	103.79	157.68	211.48	263.94	314.45	362.71	408.60	452.06	493.13	531.87	568.36
0.4	0.016	47.51	92.27	140.20	188.58	236.24	282.59	327.32	370.25	411.31	450.46	487.73	523.14
0.46	0.018	43.33	83.05	126.10	169.95	213.52	256.24	297.77	337.95	376.66	413.85	449.50	483.63
0.6	0.02	39.92	75.50	114.48	154.50	194.55	234.07	272.75	310.40	346.89	382.17	416.19	448.94
0.66	0.022	37.09	69.19	104.72	141.47	178.46	215.17	251.29	286.63	321.07	354.52	386.96	418.32
0.8	0.024	34.71	63.83	96.41	130.32	164.63	198.86	232.69	265.93	298.47	330.21	361.11	391.13

200 m⁻¹		time (min)											
δ/λx	d	6	10	16	20	26	30	36	40	46	60	66	80
0.06	0.002	289.05	500.41	629.40	710.41	764.91	804.41	835.00	859.93	881.02	899.35	915.60	930.20
0.1	0.004	176.11	348.34	477.49	581.03	660.50	721.92	770.04	808.42	839.62	865.50	887.40	906.27
0.16	0.006	127.70	258.19	374.97	474.63	558.28	628.07	686.30	735.02	775.99	810.68	840.28	865.75
0.2	0.008	100.86	206.43	306.60	396.96	476.85	546.84	607.87	661.02	707.32	747.71	783.05	814.05
0.26	0.01	83.66	171.72	258.44	339.44	413.50	480.49	540.71	594.68	642.95	686.12	724.73	759.31
0.3	0.012	71.65	146.81	222.80	295.53	363.60	426.57	484.42	537.34	585.64	629.65	669.72	706.21
0.36	0.014	62.76	128.04	195.38	261.02	323.53	382.32	437.21	488.22	535.49	579.19	619.55	656.79
0.4	0.016	55.88	113.34	173.62	233.21	290.72	345.52	397.32	446.06	491.76	534.50	574.41	611.65
0.46	0.018	50.40	101.51	155.91	210.32	263.40	314.50	363.30	409.66	453.54	494.97	534.01	570.76
0.6	0.02	45.92	91.76	141.20	191.14	240.30	288.02	333.98	377.99	419.98	459.93	497.85	533.81
0.66	0.022	42.21	83.60	128.79	174.84	220.52	265.19	308.50	350.25	390.35	428.75	465.44	500.43
0.8	0.024	39.07	76.64	118.16	160.80	203.38	245.28	286.14	325.76	364.03	400.87	436.27	470.21

260 m⁻¹		time (min)											
δ&x	d	6	10	16	20	26	30	36	40	46	60	66	80
0.06	0.002	330.90	544.18	661.83	732.41	779.81	814.93	842.85	866.11	886.12	903.70	919.40	933.59
0.1	0.004	206.83	392.47	530.72	630.81	703.77	758.10	799.69	832.51	859.21	881.54	900.66	917.39
0.16	0.006	150.48	300.75	428.27	531.81	614.83	681.36	734.96	778.54	814.39	844.26	869.48	891.11
0.2	0.008	118.51	242.38	355.24	453.10	536.46	606.95	666.46	716.77	759.46	795.86	827.08	854.05
0.26	0.01	97.78	202.25	301.83	391.90	471.74	541.82	603.05	656.46	703.05	743.76	779.41	810.72
0.3	0.012	83.19	172.99	261.36	343.69	418.74	486.40	547.04	601.21	649.52	692.60	731.04	765.37
0.36	0.014	72.32	150.69	229.71	304.96	375.01	439.44	498.30	551.86	600.47	644.54	684.47	720.66
0.4	0.016	63.89	133.10	204.28	273.25	338.49	399.44	455.98	508.16	556.20	600.33	640.83	677.99
0.46	0.018	57.16	118.85	183.39	246.82	307.60	365.11	419.09	469.51	516.45	560.05	600.50	637.97
0.6	0.02	51.64	107.07	165.93	224.46	281.17	335.38	386.78	435.25	480.80	523.50	563.46	600.80
0.66	0.022	47.07	97.15	151.10	205.31	258.32	309.43	358.30	404.76	448.77	490.34	529.54	566.45
0.8	0.024	43.19	88.68	138.34	188.71	238.35	286.58	333.03	377.50	419.90	460.23	498.48	534.75

Fig. 2. View of zones 1, 2 and 3 of the design tables for different section sizes.

In step 2, a search has been made for articles that reflect the behaviour of the density ρ, specific heat cp, emissivity ε, etc. of the pultruded FRP materials up to the limit temperature obtained in step 1. Correia et al. (2015) say that the thermo-physical properties (density, specific heat and thermal conductivity) are stable up to the decomposition temperature of the material (Td). Morgado et al. (2018a, b, c, d) say that the emissivity can also be considered constant and with a value of 0.75 up to the decomposition temperature of the material (Td).

In step 3, the equation used in Eurocode 3 part 1–2 for steel (Eq. 2) has been used to calculate the temperature in the section, but with the data corresponding to the FRP material. This equation is valid for the fire test curve ISO 834 (1999), according to which the gases follow a time-temperature curve presented below (Eq. 3).

$$\Delta\theta_{a,t} = \frac{\lambda_{\mathrm{p}} \mathrm{A}_{\mathrm{p}}/V(\theta_{g,t} - \theta_{a,t})}{d_p c_a \rho_a (1 + \varnothing/3)} \Delta t - (e^{\varnothing/10} - 1)\Delta\theta_{g,t} \tag{2}$$

$$\theta_{\mathrm{g}} = 20 + 345 \cdot \log(8\mathrm{t} + 1) \tag{3}$$

where t is expressed in minutes and θg in ºC.

On the other hand, a search has been carried out for articles where there are results of the temperatures in the sections after being subjected to this fire test ISO 834 (1999). In the tables made in this article, the data presented by Morgado et al. (2018a, b, c, d) corresponding to the type of protection Rock wool boards have been used.

The actual temperatures of the trials (θe) conducted by these authors have been compared with the results that would be obtained with the above equation (Eq. 2).

Finally, a correction coefficient (CFRP) has been applied to the equation (Eq. 2) with which the minimum quadratic error (Eq. 4) is obtained. In this way the equation (Eq. 2) will look like this (Eq. 5):

$$ECM(\theta) = \sum (\theta_e - \theta_{eq.5})^2 \tag{4}$$

$$\Delta\theta_{FRP,t} = \left[\frac{\lambda_p A_p / V(\theta_{g,t} - \theta_{FRP,t})}{d_p c_{FRP} \rho_{FRP}(1 + \varnothing/3)} \Delta t - (e^{\varnothing/10} - 1)\Delta\theta_{g,t}\right] \times c_{FRP} \tag{5}$$

In step 4, another article search has been carried out to obtain the equations proposed so far that determine the tensile, shear, longitudinal compression and transverse compression strengths as a function of section temperature for FRP material.

The equations finally used due to their lower "absolute mean percentage errors" (AMPE) have been that of Wang et al. (2011) (Eq. 6) for traction and compression, and that of Correia et al. (2013) (Eq. 7) for shear.

$$P(T) = P_u \times \left[A - \frac{(T - B)^n}{C}\right] \tag{6}$$

$$P(T) = \left(1 - e^{Be^{C \times T}}\right) \times (P_u - P_r) + P_r \tag{7}$$

in which P is the mechanical property with temperature T, Pu is the property at ambient temperature, Pr is the mechanical property after glass transition and coefficients A, B, C and n can be estimated for different temperature ranges.

Finally, in step 5, Eq. (5) has been combined with Eqs. (6) and (7) in each case to make the design tables proposed in this article for FRP profiles with different section sizes, different fire exposure times and different thicknesses of protection Rock wool boards.

3 Results

Figure 3 shows some of the design tables that have resulted from the implementation of the methodology presented in the previous section, specifically those for sections with a mass of 30 m^{-1}.

These tables give us the result of the insulation thickness that would have to be placed in the sections to achieve a reduction in the tensile, shear and compressive strength that is less than the limit obtained after making the structural calculation (in an extraordinary fire situation).

That is, the input data for these tables are the time of exposure to fire required by the structure and the minimum resistances required. And the output data would be the minimum necessary Rock wool boards insulation thickness.

TENSILE STRENGTH (oversized coefficients)

$30\ m^{-1}$		time (min)											
δ/λπ	d	5	10	15	20	25	30	35	40	45	50	55	60
0.05	0.002	0.88	0.72	0.55	0.39	0.24	0.09	-0.04	-0.16	-0.27	-0.38	-0.47	-0.56
0.1	0.004	0.94	0.85	0.76	0.66	0.57	0.47	0.38	0.29	0.20	0.12	0.04	-0.04
0.15	0.006	0.96	0.90	0.84	0.77	0.70	0.63	0.56	0.49	0.43	0.36	0.30	0.23
0.2	0.008	0.97	0.93	0.88	0.83	0.77	0.72	0.66	0.61	0.55	0.50	0.45	0.40
0.25	0.01	0.98	0.94	0.90	0.86	0.82	0.77	0.73	0.68	0.64	0.59	0.55	0.50
0.3	0.012	0.98	0.95	0.92	0.88	0.85	0.81	0.77	0.73	0.69	0.66	0.62	0.58
0.35	0.014	0.99	0.96	0.93	0.90	0.87	0.84	0.80	0.77	0.74	0.70	0.67	0.63
0.4	0.016	0.99	0.97	0.94	0.91	0.89	0.86	0.83	0.80	0.77	0.74	0.71	0.68
0.45	0.018	0.99	0.97	0.95	0.92	0.90	0.87	0.85	0.82	0.79	0.77	0.74	0.71
0.5	0.02	0.99	0.97	0.95	0.93	0.91	0.89	0.86	0.84	0.82	0.79	0.77	0.74
0.55	0.022	0.99	0.98	0.96	0.94	0.92	0.90	0.88	0.86	0.83	0.81	0.79	0.76
0.6	0.024	0.99	0.98	0.96	0.95	0.93	0.91	0.89	0.87	0.85	0.83	0.81	0.78

SHEAR STRENGTH (oversized coefficients)

$30\ m^{-1}$		time (min)											
δ/λπ	d	5	10	15	20	25	30	35	40	45	50	55	60
0.05	0.002	0.98	0.16	0.11	0.11	0.11	0.11	0.11	0.11	0.11	0.11	0.11	0.11
0.1	0.004	1.00	0.87	0.26	0.12	0.11	0.11	0.11	0.11	0.11	0.11	0.11	0.11
0.15	0.006	1.00	1.00	0.75	0.30	0.15	0.12	0.11	0.11	0.11	0.11	0.11	0.11
0.2	0.008	1.00	1.00	0.97	0.66	0.31	0.17	0.13	0.11	0.11	0.11	0.11	0.11
0.25	0.01	1.00	1.00	1.00	0.91	0.59	0.31	0.18	0.13	0.12	0.11	0.11	0.11
0.3	0.012	1.00	1.00	1.00	0.99	0.83	0.53	0.31	0.19	0.14	0.12	0.11	0.11
0.35	0.014	1.00	1.00	1.00	1.00	0.95	0.75	0.49	0.30	0.20	0.15	0.13	0.12
0.4	0.016	1.00	1.00	1.00	1.00	0.99	0.90	0.68	0.46	0.30	0.20	0.16	0.13
0.45	0.018	1.00	1.00	1.00	1.00	1.00	0.97	0.84	0.63	0.43	0.29	0.21	0.16
0.5	0.02	1.00	1.00	1.00	1.00	1.00	0.99	0.93	0.77	0.58	0.41	0.28	0.21
0.55	0.022	1.00	1.00	1.00	1.00	1.00	1.00	0.97	0.88	0.72	0.54	0.39	0.28
0.6	0.024	1.00	1.00	1.00	1.00	1.00	1.00	0.99	0.94	0.83	0.67	0.50	0.37

COMPRESIVE STRENGTH L (oversized coefficients)

$30\ m^{-1}$		time (min)											
δ/λπ	d	5	10	15	20	25	30	35	40	45	50	55	60
0.05	0.002	0.56	0.16	0.07	0.00	0.00	0.00	0.00	0.00	0.00	0.00	0.00	0.00
0.1	0.004	0.79	0.45	0.23	0.07	0.08	0.00	0.00	0.00	0.00	0.00	0.00	0.00
0.15	0.006	0.86	0.64	0.40	0.25	0.13	0.02	0.07	0.05	0.00	0.00	0.00	0.00
0.2	0.008	0.90	0.74	0.55	0.37	0.26	0.16	0.07	-0.01	0.07	0.06	0.00	0.00
0.25	0.01	0.93	0.80	0.65	0.48	0.35	0.26	0.18	0.10	0.03	-0.03	0.07	0.06
0.3	0.012	0.94	0.84	0.71	0.57	0.43	0.33	0.26	0.19	0.12	0.06	0.00	0.08
0.35	0.014	0.95	0.86	0.76	0.64	0.52	0.40	0.32	0.25	0.19	0.14	0.08	0.03
0.4	0.016	0.96	0.88	0.79	0.69	0.58	0.47	0.38	0.31	0.25	0.20	0.15	0.10
0.45	0.018	0.97	0.90	0.82	0.73	0.64	0.54	0.43	0.36	0.30	0.25	0.20	0.15
0.5	0.02	0.97	0.91	0.84	0.76	0.68	0.59	0.50	0.41	0.35	0.29	0.25	0.20
0.55	0.022	0.98	0.92	0.86	0.79	0.71	0.63	0.55	0.46	0.39	0.33	0.29	0.24
0.6	0.024	0.98	0.93	0.87	0.81	0.74	0.67	0.59	0.51	0.43	0.37	0.32	0.28

Fig. 3. Example of design tables for massiveness 30 m^{-1}.

In addition, these tables will indicate the zone (zone 1, 2 or 3) in which the section would be located (in reference to what was explained in the previous section), in case it turns out that the structure has to work in zone 2 and therefore it is necessary to make an adjustment of the modulus of elasticity following the corresponding equation (Eq. 1).

4 Analysis of the Results

Figure 4 shows the behaviour of shear strength. Three variables have been represented, the first is insulation thickness (0.002 m, 0.008 m, 0.016 m and 0.024 m), the second is section size (30 m^{-1}, 150 m^{-1} and 300 m^{-1}) and the third is fire exposure time (5 min, 10 min, 15 min, 20 min, 25 min, 30 min, 35 min, 40 min, 45 min, 50 min, 55 min and 60 min).

The behaviour according to the insulation thickness is reflected for the same section size (square = 30 m^{-1}, triangular = 150 m^{-1} or round = 300 m^{-1}) by the different colours (blue = 0.002 m, red = 0.008 m, green = 0.016 m and purple = 0.024 m). The greater the thickness of the insulation, the longer the section can withstand its initial properties (at room temperature).

The behaviour according to the size of the section is reflected for the same thickness of insulation (blue = 0.002 m, red = 0.008 m, berm = 0.016 m and purple = 0.024 m) by the different shapes (square = 30 m^{-1}, triangular = 150 m^{-1} or round = 300 m^{-1}). The larger the size of the section, the longer the section with its initial properties (at room temperature) will last.

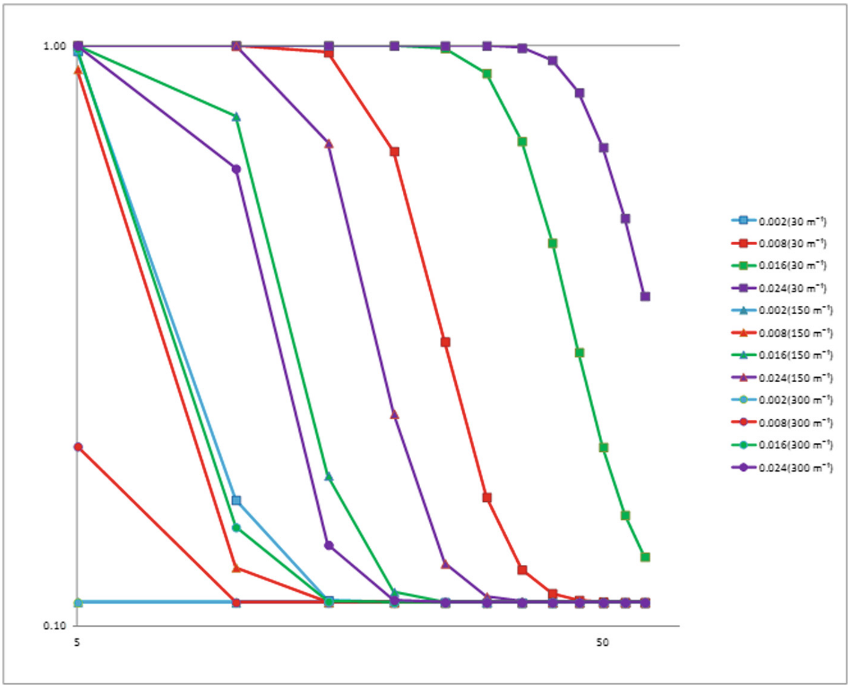

Fig. 4. Shear strength behavior.

An example of how this design methodology should be applied is described below. A beam of a simply supported slab with a span of 8 m will be calculated. Distance between beams 0.85 m, slab weight + pavement 4 KN/m^2, service overload 3 KN/m^2.

Figure 5 shows a summary of the calculation and optimisation of the beam for a persistent situation and the real stresses and minimum oversize coefficients for the extraordinary fire situation.

In Fig. 6 and using the design tables set out in this article, the minimum thicknesses required are 0.01 m and 0.022 m for the fire exposure times of 5 and 10 min respectively. It can also be seen that in both cases we are in zone 1 (green), so there is no need to update the modulus of elasticity. Finally, it is concluded that in this case it is not possible to go beyond the 10 min of exposure to fire.

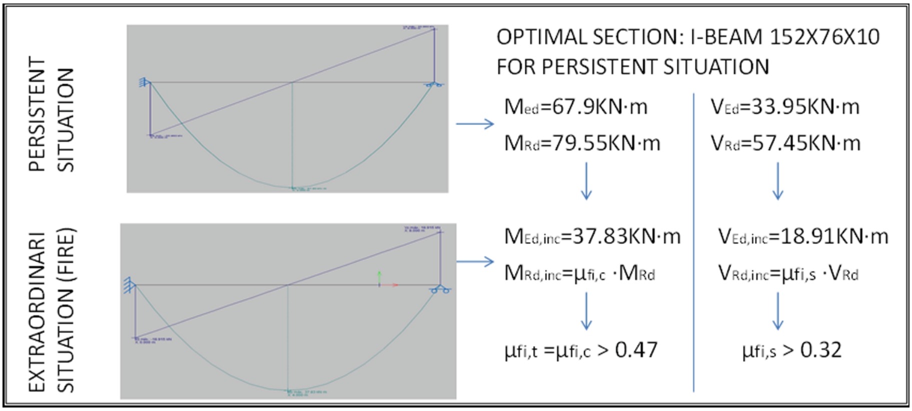

Fig. 5. Design moments and shears and resistant to persistent and extraordinary situations (fire).

I-BEAM 152X76X10 → Massivity ≈ 200 m^{-1} { RF 5 min → Esp = 0.01 m; RF 10 min → Esp = 0.022 m; RF 15 min → No se puede

COMPRESIVE STRENGTH L (oversized coefficients)

200 m⁻¹		time (min)											
d/λp	d	5	10	15	20	25	30	35	40	45	50	55	60
0.05	0.002	0.00	0.00	0.00	0.00	0.00	0.00	0.00	0.00	0.00	0.00	0.00	0.00
0.1	0.004	0.05	0.00	0.00	0.00	0.00	0.00	0.00	0.00	0.00	0.00	0.00	0.00
0.15	0.006	0.23	0.00	0.00	0.00	0.00	0.00	0.00	0.00	0.00	0.00	0.00	0.00
0.2	0.008	0.35	0.08	0.00	0.00	0.00	0.00	0.00	0.00	0.00	0.00	0.00	0.00
0.25	0.01	0.47	0.06	0.00	0.00	0.00	0.00	0.00	0.00	0.00	0.00	0.00	0.00
0.3	0.012	0.58	0.15	0.07	0.00	0.00	0.00	0.00	0.00	0.00	0.00	0.00	0.00
0.35	0.014	0.65	0.23	-0.02	0.00	0.00	0.00	0.00	0.00	0.00	0.00	0.00	0.00
0.4	0.016	0.71	0.29	0.05	0.06	0.00	0.00	0.00	0.00	0.00	0.00	0.00	0.00
0.45	0.018	0.76	0.35	0.12	0.08	0.00	0.00	0.00	0.00	0.00	0.00	0.00	0.00
0.5	0.02	0.80	0.40	0.17	-0.01	0.05	0.00	0.00	0.00	0.00	0.00	0.00	0.00
0.55	0.022	0.83	0.47	0.22	0.05	0.07	0.00	0.00	0.00	0.00	0.00	0.00	0.00
0.6	0.024	0.86	0.53	0.27	0.10	0.08	0.05	0.00	0.00	0.00	0.00	0.00	0.00

SHEAR STRENGTH (oversized coefficients)

200 m⁻¹		time (min)											
d/λp	d	5	10	15	20	25	30	35	40	45	50	55	60
0.05	0.002	0.11	0.11	0.11	0.11	0.11	0.11	0.11	0.11	0.11	0.11	0.11	0.11
0.1	0.004	0.12	0.11	0.11	0.11	0.11	0.11	0.11	0.11	0.11	0.11	0.11	0.11
0.15	0.006	0.25	0.11	0.11	0.11	0.11	0.11	0.11	0.11	0.11	0.11	0.11	0.11
0.2	0.008	0.60	0.11	0.11	0.11	0.11	0.11	0.11	0.11	0.11	0.11	0.11	0.11
0.25	0.01	0.89	0.12	0.11	0.11	0.11	0.11	0.11	0.11	0.11	0.11	0.11	0.11
0.3	0.012	0.99	0.16	0.11	0.11	0.11	0.11	0.11	0.11	0.11	0.11	0.11	0.11
0.35	0.014	1.00	0.25	0.11	0.11	0.11	0.11	0.11	0.11	0.11	0.11	0.11	0.11
0.4	0.016	1.00	0.40	0.12	0.11	0.11	0.11	0.11	0.11	0.11	0.11	0.11	0.11
0.45	0.018	1.00	0.59	0.14	0.11	0.11	0.11	0.11	0.11	0.11	0.11	0.11	0.11
0.5	0.02	1.00	0.77	0.18	0.11	0.11	0.11	0.11	0.11	0.11	0.11	0.11	0.11
0.55	0.022	1.00	0.89	0.24	0.12	0.11	0.11	0.11	0.11	0.11	0.11	0.11	0.11
0.6	0.024	1.00	0.96	0.34	0.13	0.11	0.11	0.11	0.11	0.11	0.11	0.11	0.11

Fig. 6. Minimum insulation thicknesses required according to design tables proposed in this article.

5 Conclusions

– After the elaboration of the design tables and the search of the tests carried out so far, an important conclusion is that the FRP + Rock wool boards sections cannot maintain their mechanical properties for exposure times higher than 60 min.

– If the section stays between the glass transition Tg and the decomposition temperature Td, (zone 2), it is possible that the structure is correct, but the modulus of elasticity of the section must be corrected.
– The greater the thickness of the insulation, the longer the section can withstand its initial properties (at room temperature).
– The larger the section size, the longer the section with its initial properties (at room temperature) will last.
– After the calculation or dimensioning in a persistent situation and with the over-dimensioning coefficients for the extraordinary fire situation, it is immediate to obtain the necessary insulation thicknesses for each exposure time, with the tables and design presented in this article.

References

American Composites Manufactures Association (2012) Pre-standard for load & resistance factor design (LRFD) of pultruded fiber reinforced polymer (FRP) structures. Arlington, VA: ACMA:14

Ascione L, Caron JF, Godonou P et al (2016) Prospect for new guidance in the design of FRP. Support to the implementation, harmonization and future development of the Eurocodes. JRC Report EUR 27666

Bai Y, Keller T (2007) Modeling of post-fire stiffness of E-glass fiber-reinforced polyester composites. Compos A Appl Sci Manuf 38(10):2142–2153

Bai Y, Keller T (2009) Modeling of strength degradation for fiber-reinforced polymer composites in fire. J Compos Mater 43(21):2371–2385

Bai Y, Keller T, Vallée T (2008a) Modeling of stiffness of FRP composites under elevated and high temperatures. Compos Sci Technol 68(15–16):3099–3106

Bai Y, Post NL, Lesko JJ et al (2008b) Experimental investigations on temperature-dependent thermo-physical and mechanical properties of pultruded GFRP composites. Thermochim Acta 469(1–2):28–35

BUEV-Guideline (2010) Structural polymer components for building and construction. Draft, dimensioning and construction

CEN (European Communities for Standardization) (2005) EN 1993-1-1 Eurocode 3: design of steel structures-Part 1: general rules and rules for buildings

Correia JR, Bai Y, Keller T (2015) A review of the fire behaviour of pultruded GFRP structural profiles for civil engineering applications. Compos Struct 127:267–287

Correia JR, Gomes MM, Pires JM et al (2013) Mechanical behaviour of pultruded glass fibre reinforced polymer composites at elevated temperature: experiments and model assessment. Compos Struct 98:303–313

Couto C, Real PV, Lopes N et al (2015) Resistance of steel cross-sections with local buckling at elevated temperatures. J Constr Steel Res 109:101–114

Couto C, Real PV, Lopes N et al (2016) Local buckling in laterally restrained steel beam-columns in case of fire. J Constr Steel Res 122:543–556

CUR Commission C124 (2003) Fibre-Reinforced Polymers in Civil Load-Bearing Structures. Gouda, The Netherlands

Del Hormigón Estructural I (2008) EHE-08. Madrid, Ministerio de Fomento, Secretaría General Técnica

Eurocode C (2002) 1: Action on Structures Part 1–2: General actions–Actions on Structures Exposed to Fire. Brussels: Belgium: European Committee for Standardization (CEN)
Eurocode EC (1993) 3: Design of steel structures: Part 1.2, general rules–structural fire design. Brussels: European Committee for Standardization. DD ENV 1(2)
Franssen J, Zhao B, Gernay T (2016) Experimental tests and numerical modelling on slender steel columns at high temperatures. J Struct Fire Eng 7:30–40
ISO I (1999) 834: Fire resistance tests-elements of building construction. International Organization for Standardization, Geneva, Switzerland
Knobloch M, Somaini D, Pauli J et al (2012) Numerical analysis and comparative study of the cross-sectional capacity of structural steel members in fire. J Struct Fire Eng 3(1):19–36
König J, Winter S (2004) The Eurocode 5 fire part– EN 1995– 1– 2. In: Anonymous proceedings of the 8th world conference on timber engineering, Finland
Morgado T, Correia JR, Silvestre N et al (2018a) Experimental study on the fire resistance of GFRP pultruded tubular beams. Compos B Eng 139:106–116
Morgado T, Silvestre N, Correia JR (2018b) Simulation of fire resistance behaviour of pultruded GFRP beams–part I: models description and kinematic issues. Compos Struct 187:269–280
Morgado T, Silvestre N, Correia JR (2018c) Simulation of fire resistance behaviour of pultruded GFRP beams–part II: stress analysis and failure criteria. Compos Struct 188:519–530
Morgado T, Silvestre N, Correia JR et al (2018d) Numerical modelling of the thermal response of pultruded GFRP tubular profiles subjected to fire. Compos B Eng 137:202–216
National Research Council (2007) Guide for the Design and Construction of Structures made of FRP Pultruded Elements. CNR-DT 205:25-31
Prachar M, Hricak J, Jandera M et al (2016) Experiments of Class 4 open section beams at elevated temperature. Thin-Walled Struct 98:2–18
Prachar M, Jandera M, Wald F et al (2015) Lateral torsional-buckling of class 4 steel plate beams at elevated temperature: experimental and numerical comparison. J Struct Fire Eng 6:223–236
Rosa IC, Morgado T, Correia JR et al (2018) Shear behavior of GFRP composite materials at elevated temperature. J Compos Constr 22(3):04018010
Wang K, Young B, Smith ST (2011) Mechanical properties of pultruded carbon fibre-reinforced polymer (CFRP) plates at elevated temperatures. Eng Struct 33(7):2154–2161
Wong P, Davies JM, Wang YC (2004) An experimental and numerical study of the behaviour of glass fibre reinforced plastics (GRP) short columns at elevated temperatures. Compos Struct 63(1):33–43
Yu B, Till V, Thomas K (2007) Modeling of thermo-physical properties for FRP composites under elevated and high temperature. Compos Sci Technol 67(15–16):3098–3109